6

High velocity oxy-fuel (HVOF) coatings for steam oxidation protection*

Alina Agüero, Raúl Muelas and Vanessa Gonzalez

Instituto Nacional de Técnica Aeroespacial (INTA), Área de Materiales Metálicos, Ctra. Ajalvir Km. 4, 28850 Torrejón de Ardoz (Madrid), Spain

agueroba@inta.es

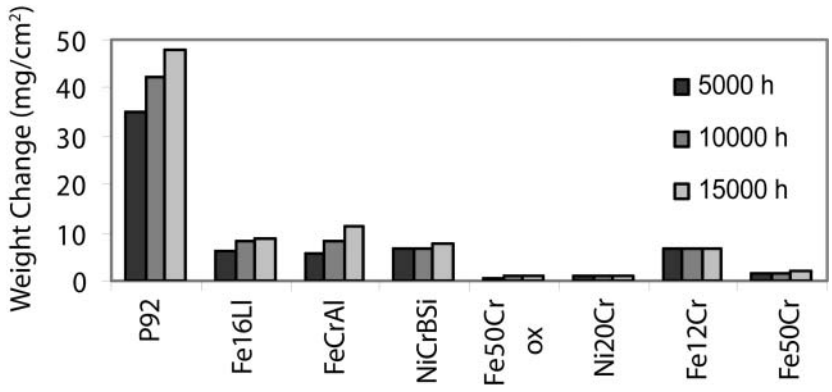
6.1 Introduction

European COST Actions 522 (completed in 2003) and 536 (ongoing) have concentrated on designing and producing steels for steam power plants capable of operating at 600–625 °C in order to increase efficiency and reduce emissions [1–4]. However, efforts to produce ferritic steels for turbine components capable of operating at temperatures of 625 °C or higher have not yet been successful [5]. Materials such as P92 and COST-developed CB2 (9 wt.% Cr) with high creep strength up to 625 °C, have unacceptable oxidation resistance (Fig. 6.1), whereas materials with higher Cr content such as COST-developed FT4 (11 wt.% Cr) have better oxidation resistance but lower creep strength. When exposed to high-pressure steam at these temperatures, ferritic steels develop thick oxides which spall after relatively few hours of exposure [6]. Cross-section reduction, blockage and component damage due to erosion caused by the spalled oxides are some of the possible consequences.

A similar situation occurred with power generation and aeronautical gas turbines 45 years ago, when efforts to develop superalloys with the required mechanical properties as well as very low oxidation rates resulted in failure at higher operating temperatures. The solution was to employ coatings on superalloys with the required mechanical properties and presently, all new generation gas turbines require high-temperature oxidation resistance coatings as well as thermal barriers [7].

In 1998, efforts to examine the feasibility of applying coatings to steam turbine components were carried out within the context of COST 522 [8]. The results were very promising and the work continued within the framework of the European Commission project 'Coatings for Supercritical Steam Cycles' (SUPERCOAT) in which eight partners from different organisations across Europe participated [9,10]. A number of coatings, applied by means of slurry deposition, pack cementation and High Velocity Oxy-Fuel (HVOF) thermal spray were subjected to a variety of tests, including steam oxidation, creep strength, thermo-mechanical fatigue, etc. The project has recently been completed and some of the explored coatings were down-selected as candidates for industrial scale application on real components and for validation.

* Reprinted from A. Agüero et al.: HVOF coatings for steam oxidation protection. *Materials and Corrosion*. 2008. Volume 59. pp. 393–401. Copyright Wiley-VCH Verlag GmbH & Co. KGaA.



6.1 Mass variation as a function of time for coated and uncoated P92 exposed to steam at 650 °C

Among the explored coating techniques, chosen on the basis of being potentially appropriate for coating large steam turbine components, HVOF thermal spray has emerged as one of the most successful. Abe and co-workers have also studied a number of HVOF deposited materials for this application [11]. This paper describes the steam oxidation behaviour of several alloyed materials deposited by this technique including the characterisation of the protective oxides formed on each material.

6.2 Experimental procedures

6.2.1 Materials

P92 (Fe: 87.69, Cr: 9.07, W: 1.79, Mn: 0.47, Mo: 0.46, V: 0.19, C: 0.12, Ni: 0.06, Nb: 0.063, N: 0.046, Si: 0.02, Al: 0.007, S: 0.006 wt.%) was obtained from Alstom Power, Switzerland. The powders employed for the deposition of coatings by HVOF are listed in Table 6.1, along with the corresponding commercial sources.

6.2.2 Coating deposition

The coatings were deposited by a Sulzer Metco Diamond Jet Hybrid HVOF unit (A-3120) mounted on a 6-axis robot (ABB) and fed by a twin rotation powder feeder.

Table 6.1 Commercial powders employed for coating deposition by HVOF

Powder (wt.%)	Source
Fe32Al	Osprey
Fe16Al	Osprey
Fe30Cr5Al1Mo1Si	Tafa-Castolín
Fe12Cr	Osprey
Fe50Cr	Osprey
Ni20Cr	Sulzer Metco
Ni17Cr4B4Si	Sulzer Metco

6.2.3 Steam oxidation testing procedure

This test was carried out in a closed loop rig including a tubular furnace with pure, flowing, re-circulating steam (shown elsewhere) [12]. Before testing, air was displaced from the chamber by means of Ar which was kept flowing while heating up to the test temperature (at approximately 600 K h^{-1}). Once at temperature, the Ar flow was closed and the steam flow was switched on. To carry out weight measurements or to remove samples, the samples were furnace cooled to about 300 °C under argon and removed from the furnace. The reheating cycle (from 300 °C to the test temperature) was also carried out under Ar. Samples were removed at different intervals of exposure for metallographic analysis.

6.2.4 Characterisation

The coatings were characterised by optical and Field Emission Gun Scanning Electron Microscope (FESEM) (JEOL JSM-6500F equipped with an Oxford INCA 200 EDX/WDX micro-analyser) examination of metallographically polished cross-sections before and after exposure as well as by electron probe micro-analysis (EPMA) (JEOL JXA-8900 equipped with an Oxford EDX micro-analyser). Phase composition was examined by X-ray diffraction (Philips X'Pert) using the Cu Kα line (15 418 nm).

6.3 Results

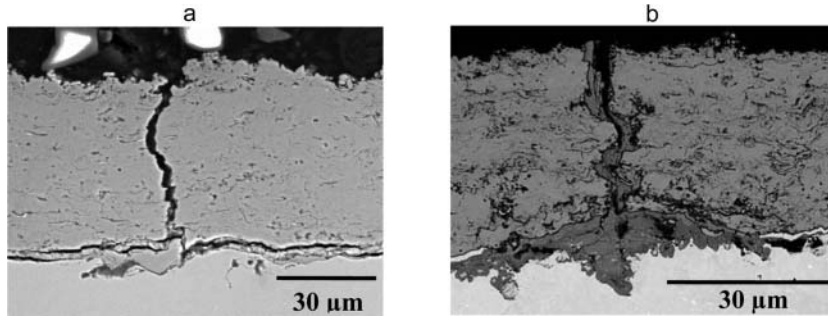
Commercially available powders of various compositions (Table 6.1) were sprayed by HVOF and optimised in order to reduce porosity and increase adhesion. The target thickness was 100–150 μm. The coatings were exposed to flowing steam at 650 °C and were characterised by FESEM and XRD before and after exposure. All coatings exhibited significantly lower mass gain than uncoated P92 when exposed to steam at 650 °C, as shown in Fig. 6.1.

6.3.1 Fe32Al

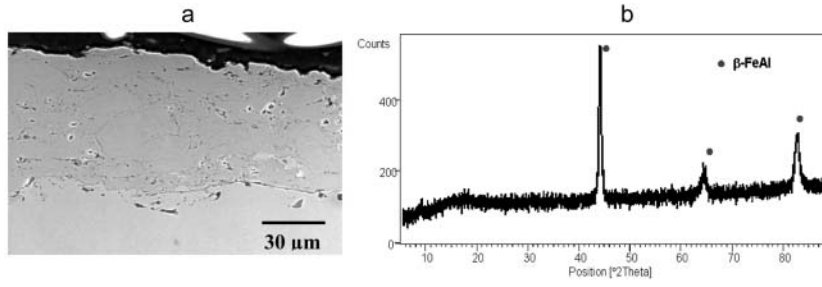
As-deposited Fe32Al (wt.%) exhibited through-thickness cracks and delamination cracks along the coating–substrate interface, causing partial coating separation (Fig. 6.2a). These cracks are similar to those observed on slurry deposited aluminide coatings [12] and probably originated due to stress caused by thermal expansion mismatch between brittle Al-rich FeAl intermetallics and the substrate. Delamination at the coating–substrate interface can be observed on exposure to steam for 1200 h; oxidation of the substrate through the above mentioned cracks occurs as shown in Fig. 6.2b. On its surface, the coating developed a mixed Al–Fe oxide which was not characterised since the coating was rejected as a candidate for protecting steam turbine components.

6.3.2 Fe16Al

In contrast to Fe32Al, Fe16Al does not develop cracks. EDX analysis and the XRD pattern indicate that β-FeAl is present (Fig. 6.3a and b). This coating exhibits excellent oxidation resistance up to at least 15 000 h despite presenting a relatively large degree of porosity obtained even after optimisation. The main phase present in a coating exposed for 10 000 h is still mostly β-FeAl, covered by a protective oxide



6.2 FESEM image of the cross-section of Fe32Al deposited by HVOF on P92: (a) as-coated and (b) after 1200 h of exposure to steam at 650 °C

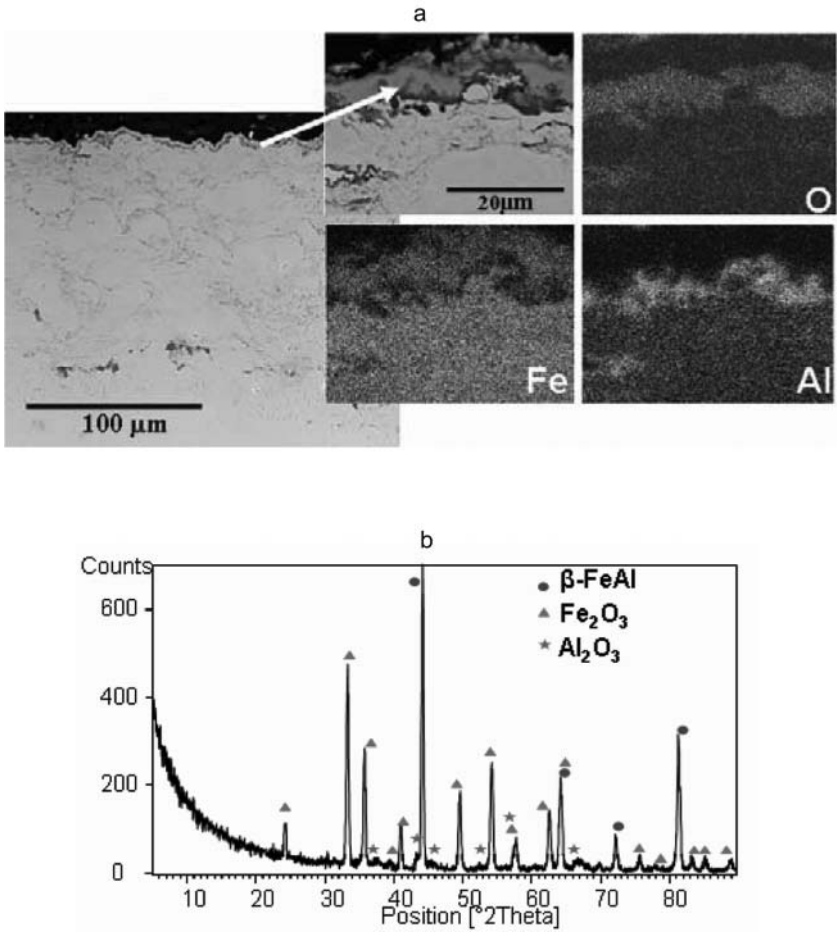


6.3 HVOF deposited Fe16Al: (a) FESEM image and (b) XRD pattern

comprising a thin inner Al-rich oxide layer with a Fe-rich oxide on top (Fig. 6.4a). EDX analysis in combination with XRD (Fig. 6.4b) indicated that this outer oxide is Fe_2O_3 (probably with some Al_2O_3 which is soluble on Fe_2O_3 [13]), while some low intensity peaks can be attributed to γ-Al_2O_3 and α-Al_2O_3, corresponding to the inner, thin, dark layer that can be observed in Fig. 6.4a. Although 650 °C is considered low for the formation of α-Al_2O_3, it has already been observed on diffusion aluminide coatings also exposed to steam at 650 °C after 10 000 h of exposure [12]. A specimen removed after 4000 h already exhibited this relatively thick bi-layered oxide (~10 µm), which does not grow significantly in up to 10 000 h of steam exposure. In addition, no significant Al depletion could be measured below this layer indicating that this is a very protective oxide under steam at 650 °C. Moreover, no coating–substrate interdiffusion was observed and therefore Al does not seem to be lost by inward diffusion, which, in contradiction, is the principal degradation mechanism observed on diffusion slurry iron aluminide coatings [9].

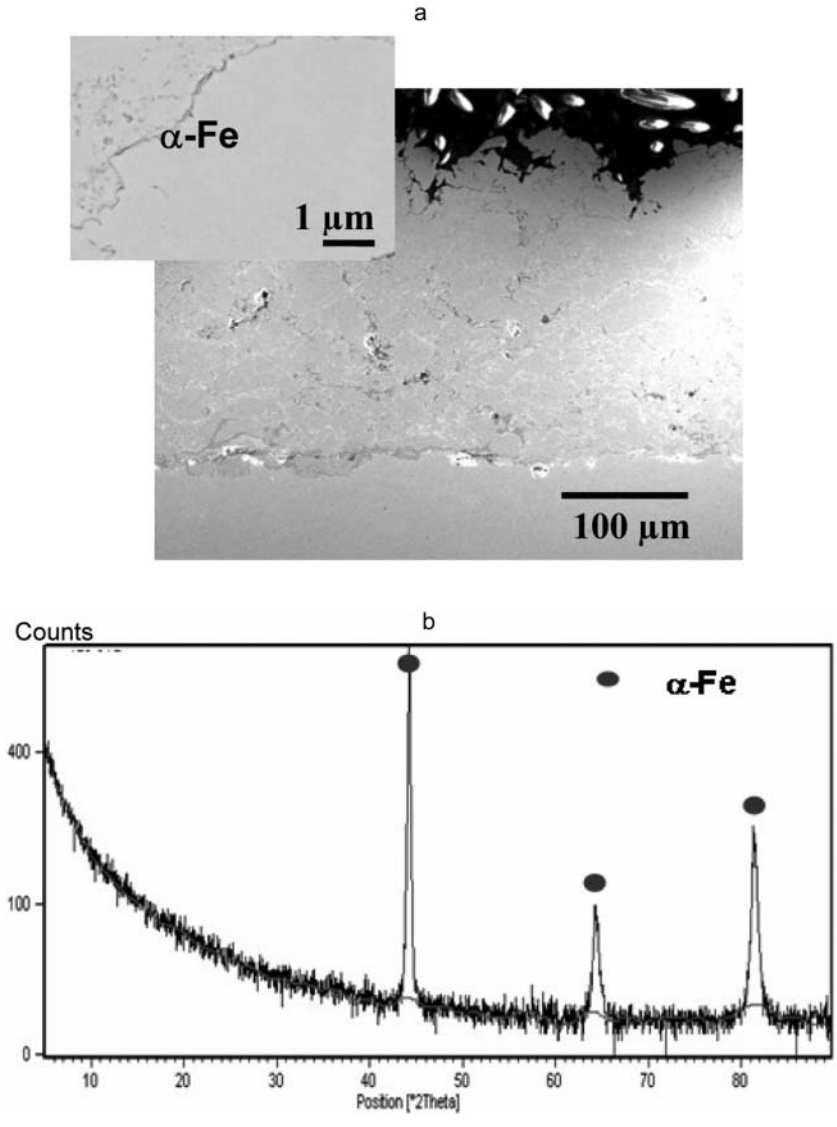
6.3.3 Fe30Cr5Al1Mo1Si

Oxidation testing results for a similar coating (without Mo and Si) exposed for times of up to 10 000 h were published previously [12]. Although the commercial source was the same, the powder batch acquired for this set of new experiments contained 1 wt.% of both Si and Mo. The 'as-deposited' layer had the same composition measured by EDX as the starting powder and a uniform microstructure exhibiting only a single phase, as shown in Fig. 6.5a. This was confirmed by XRD as only peaks attributed to α-Fe (containing Cr, Al, Mo and Si) could be observed (Fig. 6.5b). After



6.4 HVOF deposited Fe16Al exposed to steam at 650 °C for 10 000 h: (a) FESEM image and (b) XRD pattern

testing under steam at 650 °C for 10 000 h, no substrate attack could be observed and at least three phases were present within the coating (Fig. 6.6a). The dark grey phase exhibits a composition similar to that of the as-deposited coating; the light grey phase is very rich in Cr, corresponding to the σ-FeCr phase, whereas the white precipitates are very rich in Mo with a composition close to that of the $Cr_6Fe_{18}Mo_5$ phase in agreement with the XRD pattern shown in Fig. 6.7. Remarkably, no oxide layer could be observed on the surface of the coating by FESEM (even at very high magnification) in contrast to the results obtained in the earlier experiments with 'pure' Fe30Cr5Al [12]. Mikkelsen and collaborators observed that adding small amounts of Si to Fe21Cr alloys significantly reduced the growth of the Cr_2O_3 scale [14]. In Fe30Cr5Al1Mo1Si, the growth of the protective oxide may be retarded by the presence of Si to such an extent that it is not possible to observe it by SEM even after 10 000 h of exposure to steam. However, on a specimen removed after 20 000 h, some sections of the coating surface were covered with a complex oxide (Fig. 6.6b) and EDX analysis indicated the presence of Cr, Fe and Al in this oxide. The XRD patterns of both samples taken out at 10 000 and 20 000 h are very similar and

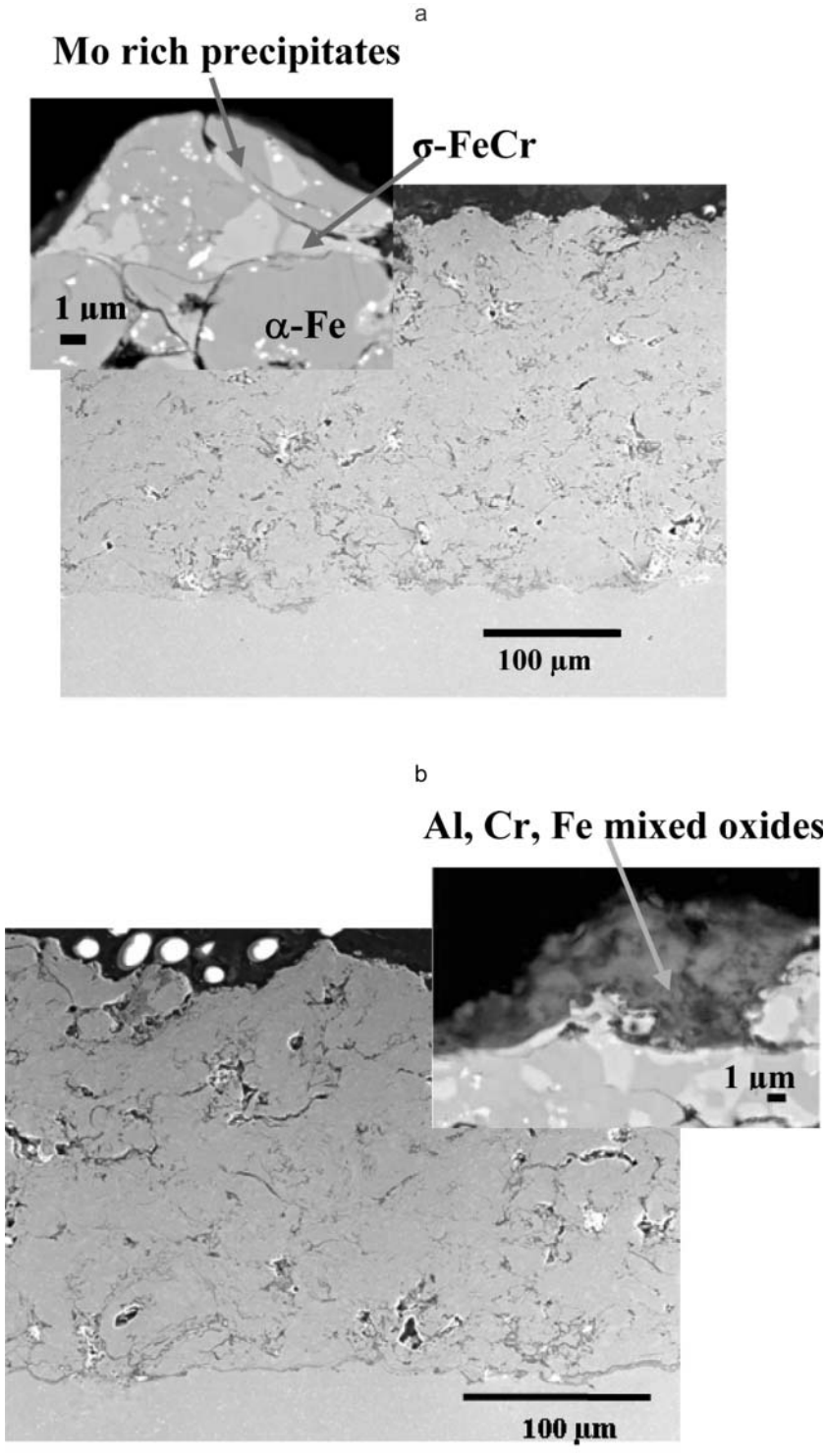


6.5 HVOF deposited Fe30Cr5Al1Mo1Si: (a) FESEM image and (b) XRD pattern

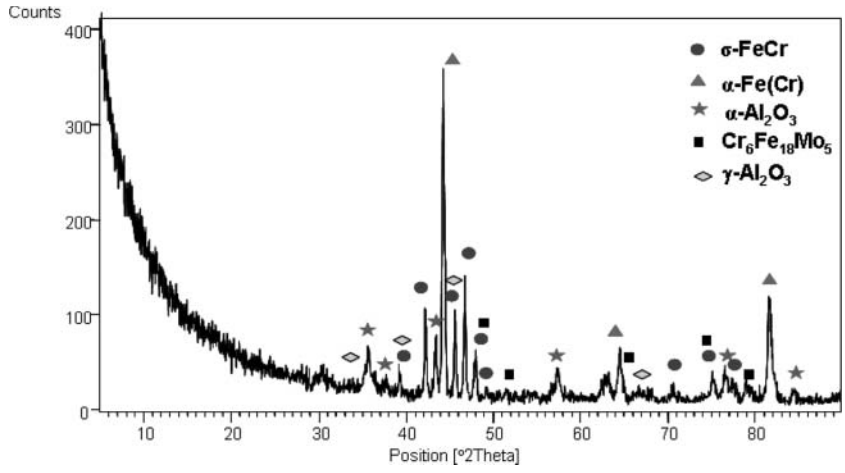
consistent with the presence of γ-Al_2O_3 and α-Al_2O_3 (Fig. 6.7). Transformation of γ-Al_2O_3 to α-Al_2O_3 may occur slowly and it is also favoured by the presence of Cr [15,16]. Some interlamellar, as well as interfacial (coating–substrate) oxidation could be observed, but without any major impact on the protective nature of the coating.

6.3.4 Fe12Cr

This low-cost powder was deposited and optimised resulting in a coating with a Cr content of 16 wt.%. XRD exhibited peaks attributed to α-Fe and some $(Fe,Cr)_3O_4$ probably resulting from partial interlamellar oxidation during spraying (Fig. 6.8a and b). After exposure to steam at 650 °C for 8100 h, the coating developed a protec-



6.6 FESEM cross-section of HVOF deposited Fe30Cr5Al1Mo1Si after: (a) 10 000 h and (b) 20 000 h of exposure to steam at 650 °C



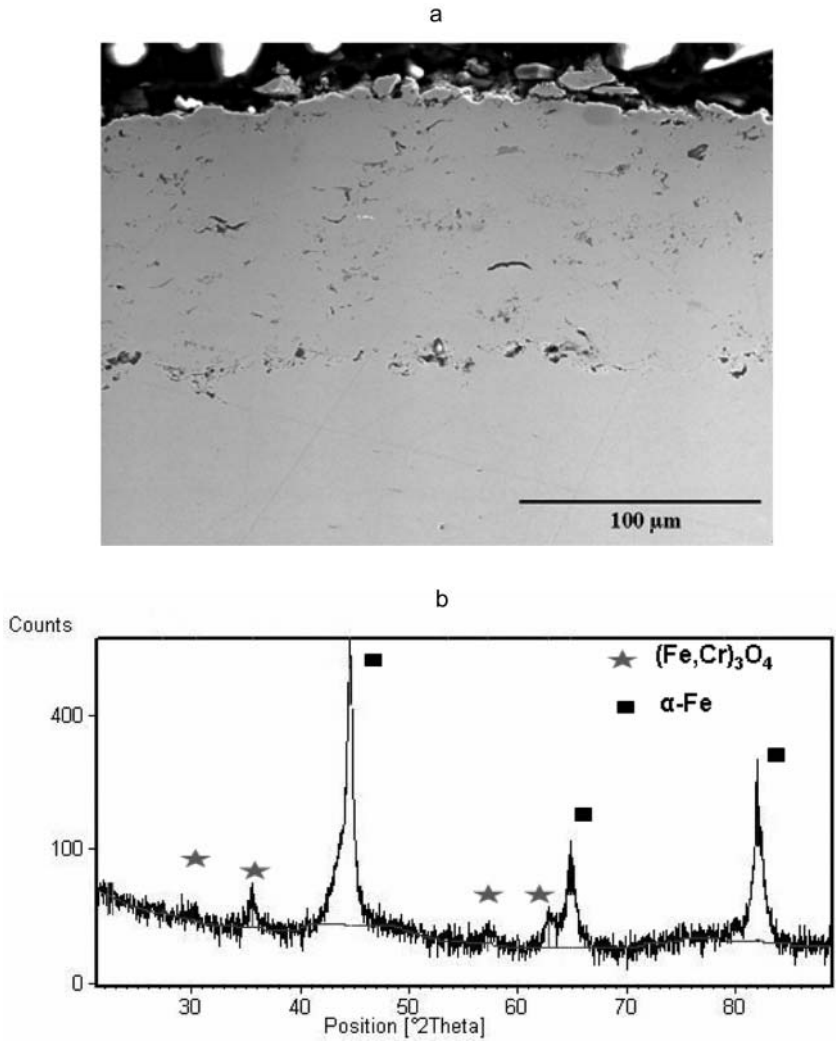
6.7 XRD pattern of HVOF deposited Fe30Cr5Al1Mo1Si after 20 000 h of exposure to steam at 650 °C

tive mixed oxide scale consisting of outer Fe,Cr oxides (mostly $(Cr,Fe)_2O_3$) on top of a thinner Cr-rich oxide, as confirmed by EDX mapping and XRD (Fig. 6.9a and b), and in agreement with results obtained for 11 wt.% Cr steels by Segerdahl *et al.* [17]. This protective scale slowly grows from ~2–3 μm after 1000 h to ~8–10 μm after 8100 h. One of the proposed mechanisms for failure of the protective scale developed by Cr-containing steels when exposed to steam at temperatures of 600 °C and higher, is the evaporation of volatile chromium oxyhydroxides [17,18]. However, in this case, at 650 °C no significant Cr depletion was measured below the scale and no evidence of evaporation was found. Moreover, there are no Fe oxide nodules, which are typical of steels with a Cr content higher than 10 wt.%, when exposed to steam at temperatures higher than 600 °C [19,20].

6.3.5 Fe50Cr

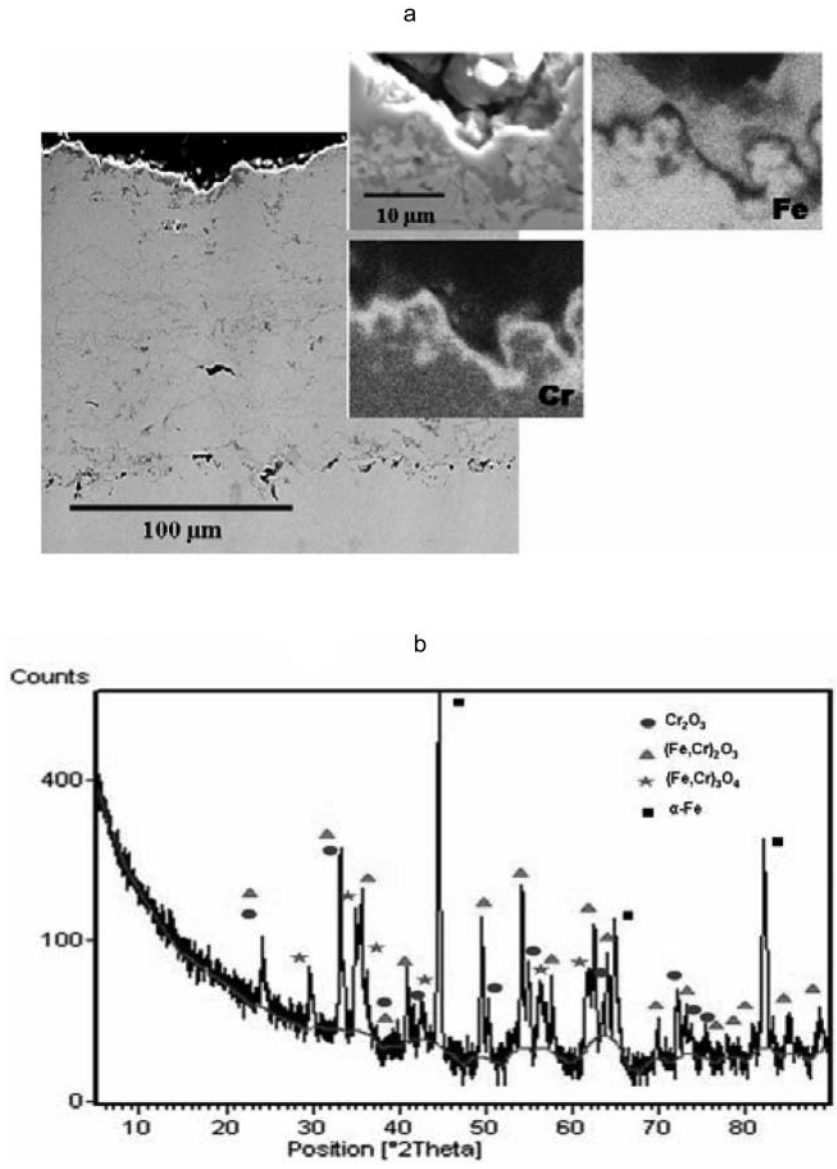
As with Fe12Cr, the as-deposited Fe50Cr coating exhibited essentially one phase (Fig. 6.10a) which, according to XRD, is a solid solution of Cr (51 wt.% as measured by EDX) in α-Fe with some $(Fe,Cr)_3O_4$. The σ-FeCr phase did not form due to rapid cooling during the spray process. After 9000 h of exposure to steam at 650 °C, two new phases could be observed (Fig. 6.10b), the darker with a very high Cr content (~60 wt.% according to EDX analysis), while the lighter and more abundant phase exhibited a much lower Cr content (~27 wt.%). Moreover, some peaks attributed to σ-FeCr were present in the XRD pattern as shown in Fig. 6.11. It appears, therefore, as if the initial 50–50 wt.% solid solution alloy has transformed into two new solid solutions, of Fe in Cr and of Cr in Fe as well as into σ-FeCr. The coating has developed a protective, very slow growing Cr_2O_3 scale which, after 9000 h, has only reached a thickness of ~2–3 μm. Again, no evidence of evaporation of volatile chromium oxyhydroxides was found and for this higher Cr coating, no Fe,Cr oxides could be observed on the surface of the coating.

In a separate set of experiments, the HVOF deposition parameters were modified so as to maximise oxidation during spraying. Indeed, significant oxidation of the powder took place resulting in a cermet coating that has been designated $FeCrO_x$,



6.8 HVOF deposited Fe12Cr: (a) FESEM image and (b) XRD pattern

composed of a $(Fe,Cr)_2O_4$ spinel on an FeCr matrix (α-Fe), as confirmed by XRD, which also exhibits peaks attributed to Cr_2O_3 (Fig. 6.12a and b). After 20 000 h of exposure to steam at 650 °C, the coating developed a protective oxide layer composed of Cr_2O_3 and 'patches' of Cr and Fe mixed oxides and the content of the oxidised phases (dark) appeared to have increased when observed by FESEM, as seen in Fig. 6.13. EDX analysis showed that the Cr content in the metallic phase had decreased to 20–30 wt.% whereas that of the oxide species had become higher. On closer observation, some of the large metallic lamella within the coating showed different phases with different Cr contents, as was observed when Fe50Cr was exposed to steam for several hours at 650 °C (see above). The XRD pattern (Fig. 6.14) exhibits two new oxide phases while the intensity of the peaks attributed to α-Fe present in the initial coating pattern has been significantly reduced. The peaks attributed to Cr_2O_3 have grown in intensity and the new peaks appear to

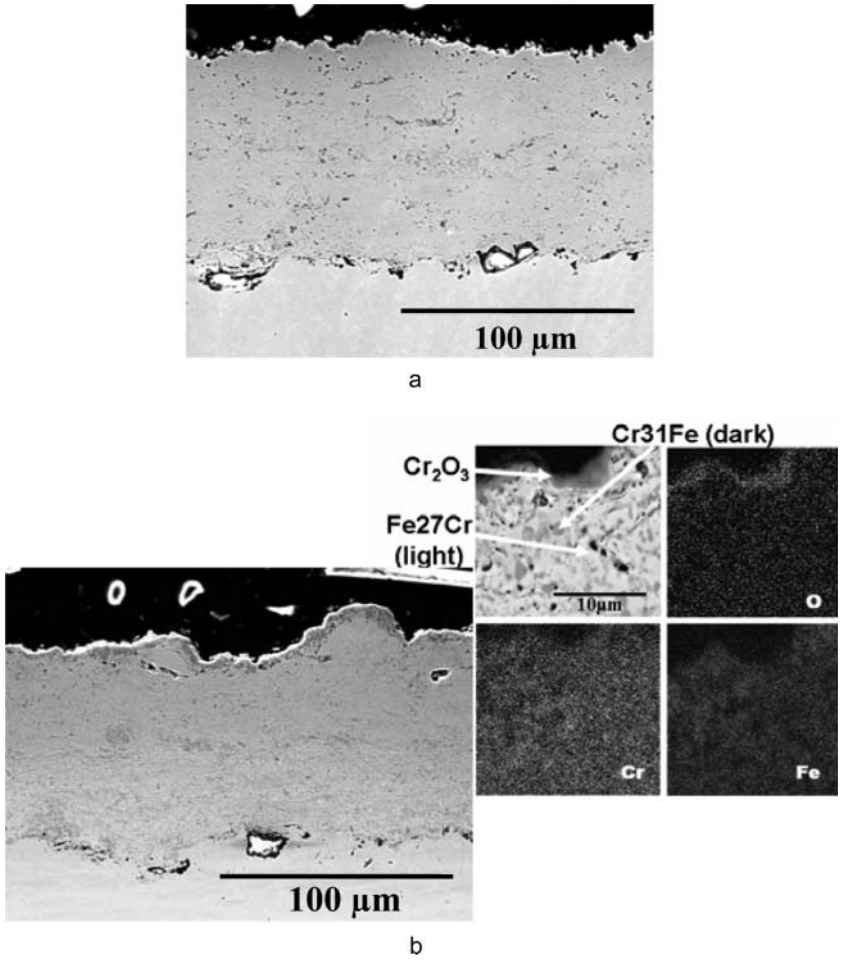


6.9 HVOF deposited Fe12Cr exposed to steam at 650 °C for 8100 h: (a) FESEM image and (b) XRD pattern

correspond to Fe_2O_3 and $(Cr,Fe)_2O_3$. Although oxidation of the metallic matrix appeared to have increased on exposure to steam, no evidence of substrate attack could be observed.

6.3.6 Ni20Cr

This coating was also studied previously by this group [8,12] for exposures up to 10 000 h and by Abe and co-workers [11,20,21] for shorter exposures but also

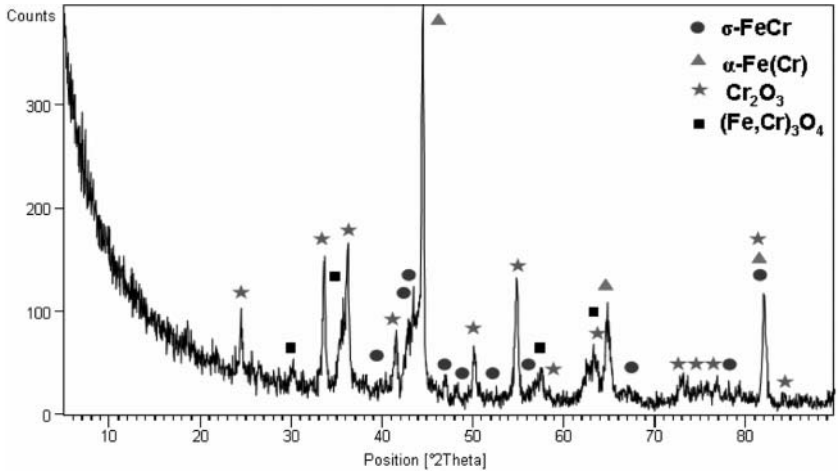


6.10 FESEM image of the cross-section of Fe50Cr deposited by HVOF on P92: (a) as-coated and (b) after 9000 h of exposure to steam at 650 °C

at other temperatures. As-deposited Ni20Cr is a single phase layer, as shown in Fig. 6.15a, corresponding to a solid solution of Cr in Ni according to XRD. Excellent behaviour has been observed for exposures up to 30 000 h (test ongoing). FESEM of the cross-section of a sample taken out after 20 000 h, showed no coating degradation or substrate attack and a very thin protective Cr_2O_3 layer on the coating surface (Fig. 6.15b). However, a small degree of coating–substrate interdiffusion could be observed with mostly outwards diffusion of Fe. XRD of this sample still indicated mostly a solid solution of Cr in Ni as well as some peaks attributed to Cr_2O_3 (Fig. 6.16). Again, no evidence of evaporation of volatile chromium oxyhydroxides was found, as no significant Cr depletion within the coating and below the scale was observed.

6.3.7 Ni17Cr4B4Si

This coating exhibited an unexpected behaviour when exposed to steam at 650 °C. After 10 000 h of exposure, the coating developed a very complex thick (~30 µm)



6.11 XRD pattern of HVOF deposited Fe50Cr after 9000 h of exposure to steam at 650 °C

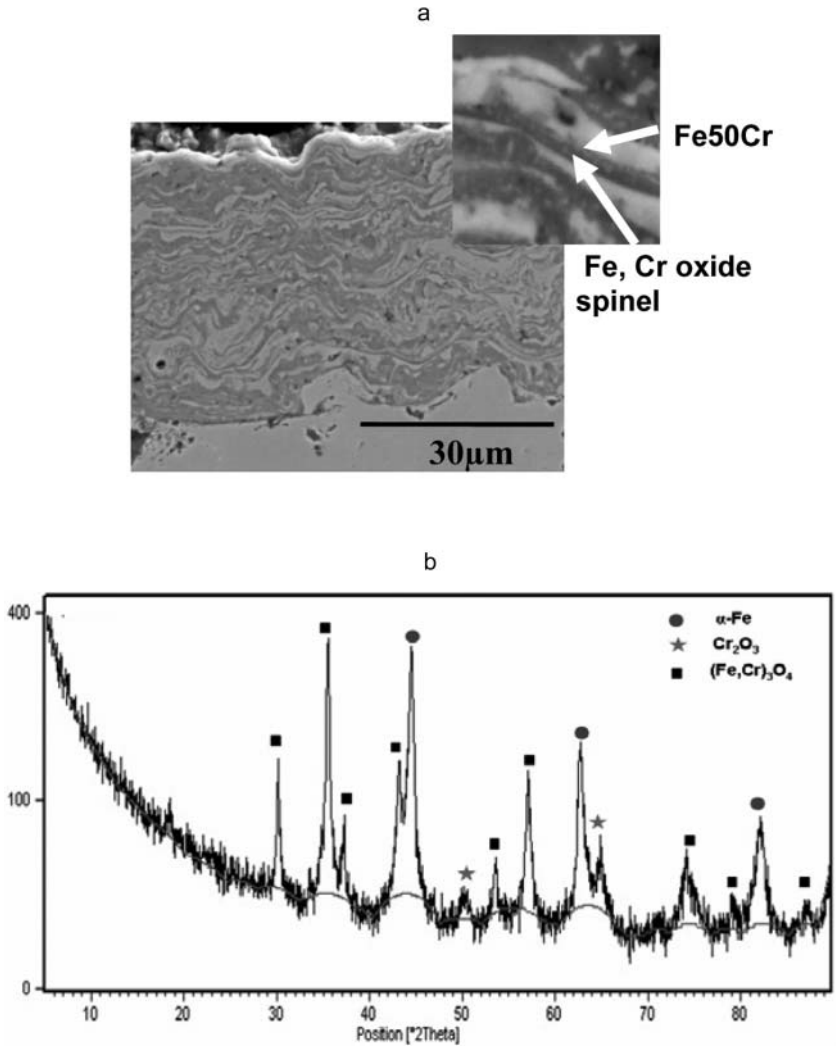
oxide containing all of its elements, as shown in Fig. 6.17. Significant B depletion under the scale was observed by EDX mapping whereas Cr and Si depletion also took place but to a minor extent. Unoxidised Ni was also present within the scale, as shown in a profile carried out by EPMA (Fig. 6.18). Despite its relatively high Cr content, this coating does not form protective Cr_2O_3 but it is nevertheless more resistant to steam at 650 °C than the uncoated substrate (Fig. 6.1).

6.4 Discussion

All of the deposited coatings showed better steam oxidation resistance than uncoated P92. Depending on their composition, pure or mixed protective oxides which were more or less stable were formed.

After several thousand hours, on Fe32Al and Fe16Al, Fe,Al mixed oxides were formed with, in the case of Fe16Al, a very thin inner layer of pure Al oxide. This layer appears to be a mixture of γ-Al_2O_3 and α-Al_2O_3 according to XRD, despite the relatively low temperature. It has already been shown that slurry diffusion Fe aluminide coatings develop α-Al_2O_3 after long time exposure to steam at 650 °C [12]. However, most results published in the literature indicate that α-Al_2O_3 does form only at temperatures higher than 850 °C but the corresponding experiments were carried out for relatively short periods of time [15,16,22]. Moreover, Boggs reported the appearance of both γ-Al_2O_3 and α-Al_2O_3 at temperatures higher than 600 °C, suggesting that α-Al_2O_3 results from recrystallisation of γ-Al_2O_3 [23]. Under the present experimental conditions, α-Al_2O_3 may also form slowly from less stable γ-Al_2O_3. On the other hand, the protective oxide formed on Fe30Cr5Al1Mo1Si exposed to steam for 10 000 h appears to be too thin to be observed by FESEM, probably due to the presence of Si. However, relatively intense peaks attributed to both γ-Al_2O_3 and α-Al_2O_3 could be observed by XRD (they may be due in part to interlamellar oxidation, typical of thermally sprayed coatings). Despite the high Cr content of the latter coating, no Cr_2O_3 was observed.

As Fe12Cr forms a mixed Cr,Fe oxide whereas Fe50Cr forms pure Cr_2O_3, the critical content of Cr required to form pure protective Cr_2O_3 in FeCr alloys must be

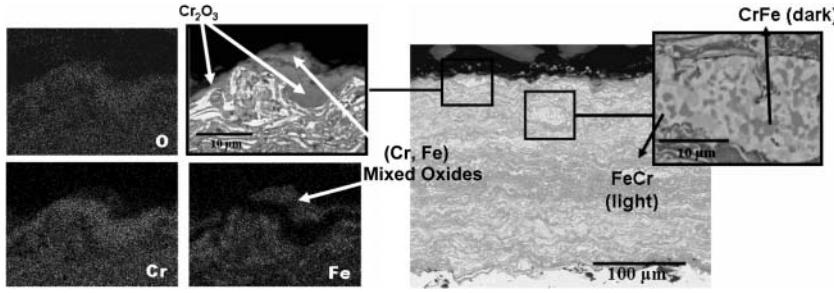


6.12 HVOF deposited FeCrOx: (a) FESEM image and (b) XRD pattern

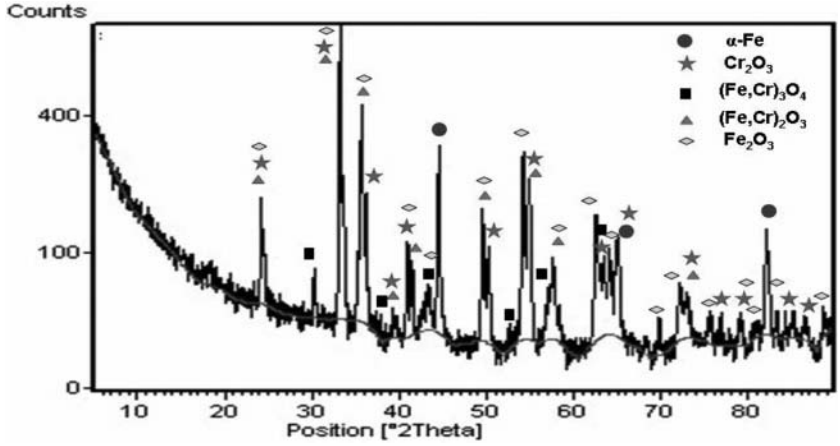
somewhere within the range of 12–50 wt.%. The endurance of Cr_2O_3 under steam at 650 °C is remarkable for Fe50Cr and Ni20Cr. In order to form the volatile species $CrO_2(OH)_2$, responsible for the volatilisation of the oxide, O_2 is needed, as shown in the following equation:

$$Cr_2O_3 + 3/2O_2 + 2H_2O \rightarrow 2CrO_2(OH)_2$$

The present experiments were performed in the absence of O_2, under a pure flowing steam, employing thoroughly de-oxygenated water (some O_2 must be present in equilibrium). A plausible explanation for the observed stability of Cr_2O_3 may be that, under the experimental conditions used in this work, $CrO_2(OH)_2$ would only form in insignificantly low amounts, if any. Moreover, no mixed oxides were observed in Fe50Cr after several thousand hours, confirming the stability of the Cr_2O_3 layer. Surprisingly, in a relatively high Cr-containing Ni-base coating such as Ni17Cr4B4Si,



6.13 FESEM image of the cross-section of HVOF deposited FeCrOx exposed to steam at 650 °C for 20 000 h

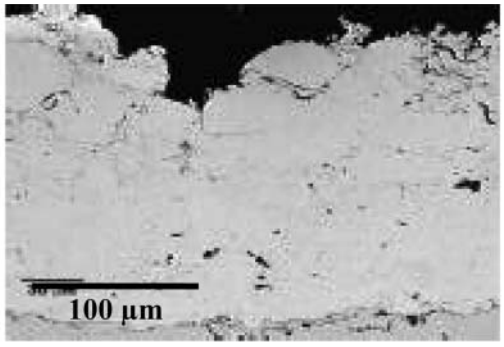


6.14 XRD pattern of HVOF deposited FeCrOx after 20 000 h of exposure to steam at 650 °C

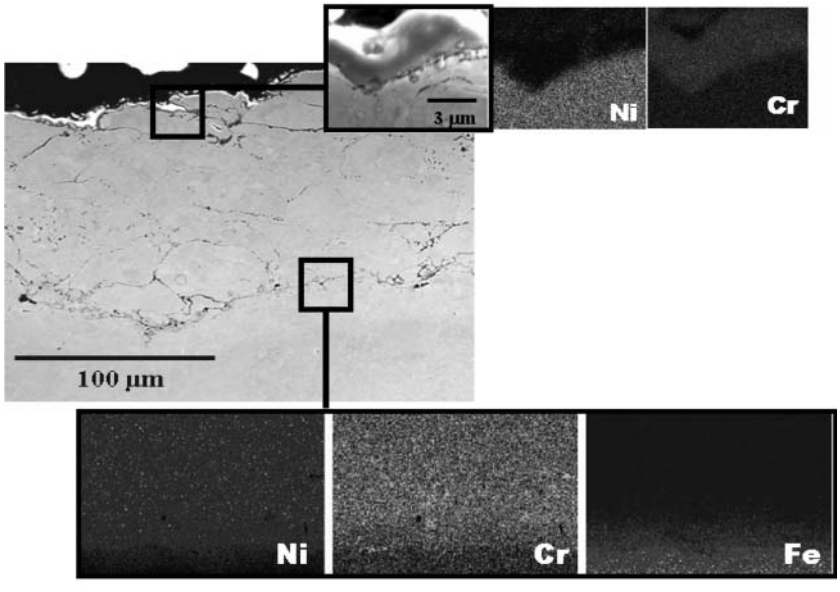
no protective Cr_2O_3 formed. Either the critical content of Cr required to form Cr_2O_3 in NiCr alloys is higher than 17 wt.% (and lower than 20 wt.%) or Si and/or B have a significant effect in preventing its formation.

6.5 Conclusions

- Several coating compositions, including protective alumina, chromia and mixed oxide formers have been deposited by HVOF. The steam oxidation resistance at 650 °C of most of these coatings is very high and will probably exceed 100 000 h (steam power plant design criteria [24]).
- Despite the relatively low test temperature used in these experiments, α-Al_2O_3 was observed on all of the studied Al-containing coatings.
- Protective Cr_2O_3 was formed on Fe50Cr and Ni20Cr and no evidence of oxide loss by Cr oxyhydroxide evaporation was found even after very long exposures to steam at 650 °C.
- A new composite Fe,Cr oxide coating has been deposited.

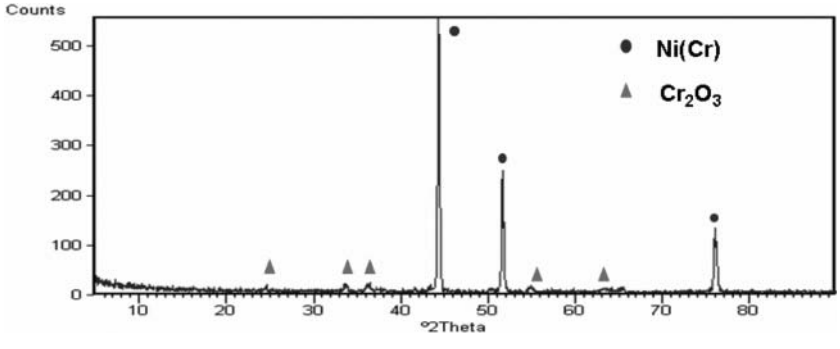


a

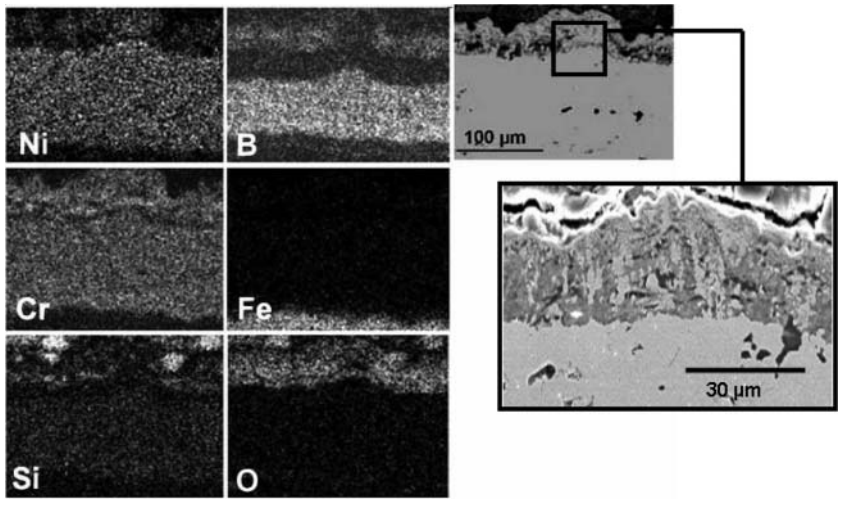


b

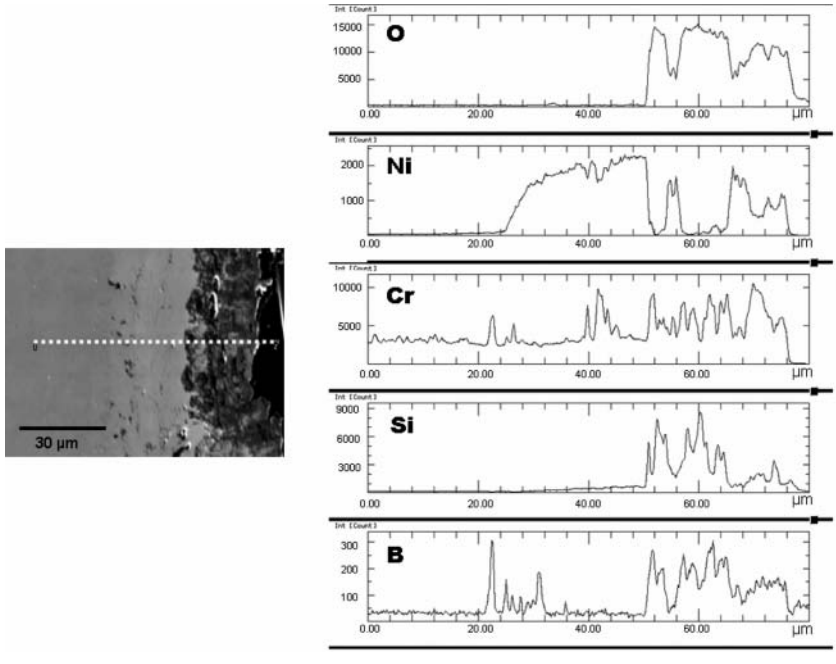
6.15 FESEM image of the cross-section of Ni20Cr deposited by HVOF on P92: (a) as-coated and (b) after 20 000 h of exposure to steam at 650 °C



6.16 XRD pattern of HVOF deposited Ni20Cr after 20 000 h of exposure to steam at 650 °C



6.17 FESEM image and EDX mapping of the cross-section of Ni17Cr4B4Si deposited by HVOF on P92 after 10 000 h of exposure to steam at 650 °C



6.18 EPMA profile of Ni17Cr4B4Si exposed to steam for 10 000 h at 650 °C

Acknowledgements

The authors are grateful to the European Commission for financial support through the SUPERCOAT project, and to P. Vallés and M. C. García Poggio for their very valuable assistance in FESEM and XRD, respectively. All of the members of the Area of Metallic Materials at INTA are also acknowledged for their support during all of the stages of this work.

References

1. T. U. Kern, M. Staubli, K. H. Meyer, K. Esher and G. Zeiler, in Proc. 7th Liege Conf., 30 Sept.–2 Oct. 2002, *Mater. Adv. Power Eng.* (2002), 1049.
2. M. Staubli, K. H. Meyer, W. Gieselbrecht, J. Stief, A. Di Gianfrancesco and T. U. Kern, in Proc. 7th Liege Conf., 30 Sept.–2 Oct. 2002, *Mater. Adv. Power Eng.* (2002), 1065.
3. T. U. Kern, M. Staubli, K. H. Meyer, B. Donth, G. Zeiler and A. Di Gianfrancesco, in Proc. 8th Liege Conf., 18–20 Sept. 2006, *Mater. Adv. Power Eng.* (2006), 843.
4. M. Staubli, R. Hanus, T. Weber, K. H. Meyer and T. U. Kern, in Proc. 8th Liege Conf., 18–20 Sept. 2006, *Mater. Adv. Power Eng.* (2006), 855.
5. J. Hald, in Proc. 8th Liege Conf., 18–20 Sept. 2006, *Mater. Adv. Power Eng.* (2006), 917.
6. W. J. Quadakkers, P. J. Ennis, J. Zurek and M. Michalik, *Mater. High Temp*., 22 (2005), 47.
7. T. Narita, T. Izumi, T. Nishimoto, Y. Shibata, K. Zaini Thosin and S. Hayashi, *Mater. Sci. Forum*, 522-523 (2006), 1.
8. A. Agüero, F. J. García de Blas, R. Muelas, A. Sánchez and S. Tsipas, *Mater. Sci. Forum*, 369-372 (2001), 939.
9. A. Agüero, R. Muelas and M. Gutiérrez, *Mater. Sci. Forum*, 522-523 (2006), 205.
10. M. B. Henderson, M. Scheefer, A. Agüero, B. Allcock, B. Norton, D. N. Tsipas and R. Durham, 'Development and validation of advanced oxidation protective coatings for super critical steam power generation plants', in Proc. 8th Liege Conf., 18–20 Sept. 2006, *Mater. Adv. Power Eng.* (2006), 1553.
11. T. Sundararajan, S. Kuroda, K. Nishida, T. Itagaki and F. Abe, *ISIJ Int.*, 44 (2004), 139.
12. A. Agüero, R. Muelas, B. Scarlin and R. Knoedler, in Proc. 7th Liege Conf., 30 Sept.–2 Oct. 2002, *Mater. Adv. Power Eng.* (2002), 1143.
13. L. M. Atlas and W. K. Sumica, *J. Am. Ceram. Soc.*, 41 (1958), 50.
14. L. Mikkelsen, S. Linderoth and J. B. Bilde-Sørensen, *Mater. Sci. Forum*, 461-462 (2004), 117.
15. P. Tomaszewicz and G. R. Wallwork, *Rev. High Temp. Mater.*, 4 (1978), 75.
16. R. Prescott and M. J. Graham, *Oxid. Met.*, 38 (1992), 73.
17. K. Segerdahl, J. E. Svensson, M. Halvarsson, I. Panas and L. G. Johansson, *Mater. High Temp.*, 21 (2005), 69.
18. H. Asterman, K. Segerdahl, J. E. Svensson, L. G. Johansson, M. Halvarsson and J. E. Tang, *Mater. Sci. Forum*, 461-464 (2004), 775.
19. W. J. Quadakkers and P. J. Ennis, in Proc. 6th Liege Conf., *Mater. Adv. Power Eng.* (1998), 123.
20. T. Sundararajan, S. Kuroda, T. Itagaki and F. Abe, in Thermal Spray 2003: Advancing the Science and Applying the Technology, 495. ASM International, Materials Park, Ohio, USA, 2003.
21. T. Sundararajan, S. Kuroda, T. Itagaki and F. Abe, *ISIJ Int.*, 43 (2003), 104.
22. G. Berthomé, E. N'Dah, Y. Wouters and A. Galerie, *Mater. Corros*., 56 (2005), 389.
23. W. E. Boggs, *J. Electrochem. Soc.*, 118 (1971), 906.
24. R. W. Vanstone, *Mater. Adv. Power Eng.* (2002), 1035.